1st International Conference on Sensing Technology
November 21-23, 2005 Palmerston North, New Zealand

Recognitions of Micro Non-Magnetic and Ferromagnetic Material with SV-GMR Sensor

Komkrit Chomsuwan, Sotoshi Yamada, Takeshi Hagino, Teerasak Somsak,
Kenhachiro Minamide, and Masayoshi Iwahara
Institute of Nature and Environmental Technology,
Kanazawa University, Kodatsuno 2-40-20, Kanazawa 920-8667, Ishikawa, Japan
komkrit@magstar.ec.t.kanazawa-u.ac.jp

Abstract

This paper describes the recognition of micro non-magnetic (conductive) and ferromagnetic material with spin-valve magneto-resistance (SV-GMR) sensor. High frequency and static magnetic fields were applied to material for the recognition of the micro conductive and ferromagnetic material respectively. The SV-GMR sensor is used to detect the magnetic field variation occurred wherever the material exists. The experimental results were carried out to detect the non-magnetic micro-bead array (PbSn, 125 μm radius) by the SV-GMR sensor and agree with analytical results based on analytical method. Furthermore, the experimental results of ferromagnetic particle (Fe, sizes of 20-60 μm) detection were also performed by the SV-GMR sensor.

Keywords: spin-valve giant magnetoresistance, conductive material, ferromagnetic material, eddy currents

1 Introduction

Recently, several kinds of magnetic sensors such as hall, magnetoresistance (MR), fluxgate, super-conducting quantum interference device (SQUID), and etc. have been successfully applied to detect cracks on conductive material based on eddy current testing (ECT) technique and also for ferromagnetic detection in bioengineering application [1-3]. Since spin valve giant magnetoresistance (SV-GMR) sensor has many advantages, such as high-sensitivity to low magnetic field (10nT-10mT) over broad range of frequency, high-spatial resolution, inexpensive, and etc., it has been applied to various fields. For electronic application, SV-GMR sensor has been applied to detect micro defects on micro conductor based on ECT technique, such as high density printed circuit board inspection [4]. Moreover, SV-GMR sensor has been proposed for utilization in biological application such as detection of ferromagnetic nano-bead, wire and magnetic label by flowing the ferromagnetic material proximity to SV-GMR sensor.

In this paper, the recognitions of non-magnetic (conductive) material based on eddy-current testing technique and of ferromagnetic material with SV-GMR sensor are proposed. The probe configuration and SV-GMR sensor characteristics are described. Microbeads (PbSn) with 100-760 μm in diameter are tested as a model for non-magnetic material detection. High frequency ECT technique with SV-GMR sensor is applied to recognize microbead. By the way, the detections of ferromagnetic particles (Fe) with sizes of 20-60 μm by SV-GMR sensor are also proposed because of the SV-GMR advantages as mentioned above although SQUID and fluxgate sensor provide higher sensitivity than SV-GMR. Ferromagnetic material detection is performed by applied static magnetic fields to ferromagnetic material.

2 SV-GMR sensor

The configuration of SV-GMR sensor used in the experiment and its characteristics are shown in figure 1. A normal resistance of the SV-GMR sensor is around 400 Ω and DC bias current is 5mA fed to the SV-GMR sensor. As shown in figure 1(b), the external magnetic fields ranged from -4 to 4 mT was applied to test the characteristics of the SV-GMR sensor in its sensing axis and the figure show that the SV-GMR has maximum MR ratio and sensitivity in linear region around 11 % and 6 %/mT respectively.

The AC characteristics at each of the SV-GMR sensor axis were tested with the magnetic fields ranged from -50 to 50 μT at the frequency of 500 kHz as shown in figure 1(c). The SV-GMR sensor has sensitivity around 5 %/mT (100 mV/mT) to the magnetic fields in the *z*-direction whereas the sensitivity in *x*- and *y*-direction has less than 1.5 %/mT (30 mV/mT) and 0.5%/mT (10 mV/mT) respectively. These mean that the SV-GMR sensor is capable of detection the magnetic field only in *z*-direction (sensing axis).

3 Non-Magnetic Material Detection

3.1 Structure of ECT Probe with SV-GMR Sensor

The structure of ECT probe consists of planar meander coil and SV-GMR sensor as shown in figure

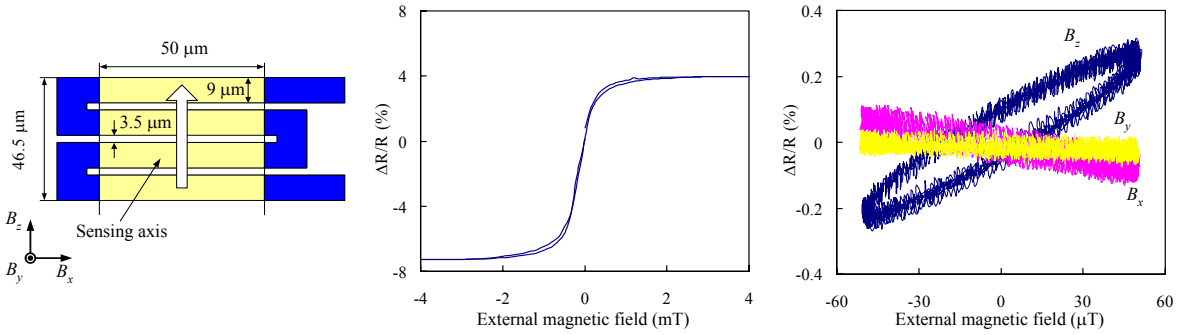

(a) Configuration. (b) DC characteristics (c) AC characteristics

Figure 1: SV-GMR configuration and its characteristics

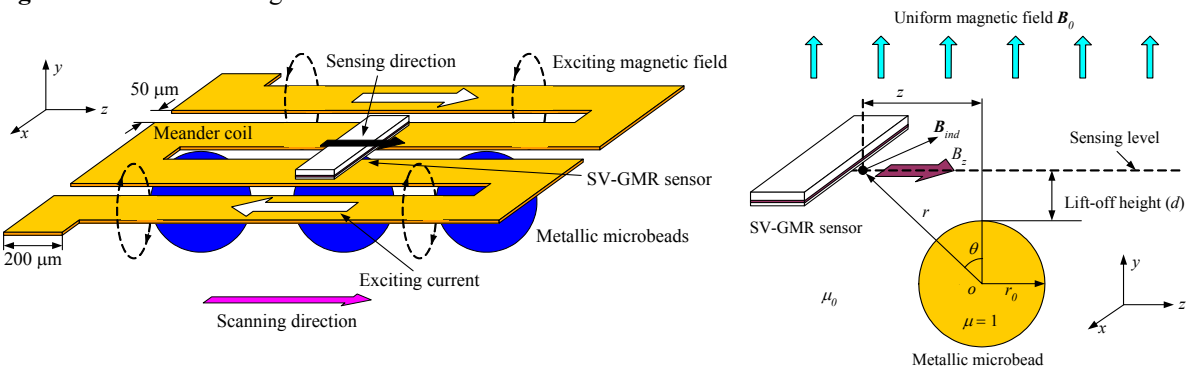

Figure 2: Proposed ECT probe structure with SV-GMR sensor (left) and magnetic field analysis model (right).

2(left). High frequency sinusoidal current was fed to planar meander coil to generate high frequency magnetic fields applied to microbead only in *x*- and *y*-axis. Eddy currents flowing in the microbead are induced by exciting magnetic fields and generates the z-axis component of magnetic fields. The SV-GMR sensor was mounted on the planar meander coil and set the sensing axis to detect magnetic fields only in z-axis that parallel with scanning direction. Because the planar meander coil with 35 μm thickness is sandwiched by two films with 100 μm thickness to separate the coil from the SV-GMR sensor and scanning surface, the distance from the SV-GMR surface to the scanning surface is at least 135 μm.

3.2 Analysis of Magnetic Field by Analytical Method

The magnetic fields generated by eddy currents flowing in the microbead were analyzed by a simple model as shown in figure 2(right). Assuming that the microbead is placed under uniform magnetic field $\boldsymbol{B_0}$, induced eddy-current flowing in the microbead is expressed as

$$J(r,\theta,\phi) = -j\omega\sigma a J_1(kr) B_0 \sin\theta \qquad (1)$$

where

$$a = \frac{r_0}{\mu_0} \frac{1}{J_1(kr_0)/\mu_0 + [kr_0 J_0(kr_0) - J_1(kr_0)]/\mu},$$

$$k = (-1+j)\sqrt{\omega\sigma\mu/2},$$

σ : conductivity of the bead (PbSn: 6.8×10^6 S/m),
μ_0, μ : permeability of air and the microbead,
J_0, J_1 : zero and first order Bessel function [5].

The magnetic field B_z at each point on sensing level is, therefore, expressed as

$$B_z = 3b\frac{z(r_0+d)}{r^5}B_0 \qquad (2)$$

where

$$b = r_0^3 \frac{J_1(kr_0)/2\mu_0 - [kr_0 J_0(kr_0) - J_1(kr_0)]/2\mu}{J_1(kr_0)/\mu_0 + [kr_0 J_0(kr_0) - J_1(kr_0)]/\mu}.$$

Analytical results show that the magnetic field distribution depends on frequency of applied magnetic fields as shown in figure 3 because high frequency magnetic fields generate high eddy current density distributed at near surface of the microbead as shown in figure 3(a).

The magnetic fields vary at the position where the conductive microbead exists at the 0 mm displacement as shown in figure 3(b). The peaks of magnetic fields occur at the outside diameter of the microbead and the maximum amplitude of magnetic field variation also depends on the microbead radius as shown in figure 3(c). The analysis of magnetic field distribution obtained from microbead array is also performed by equation (2). Magnetic field distributions obtained from each of microbead are separately calculated and they were combined

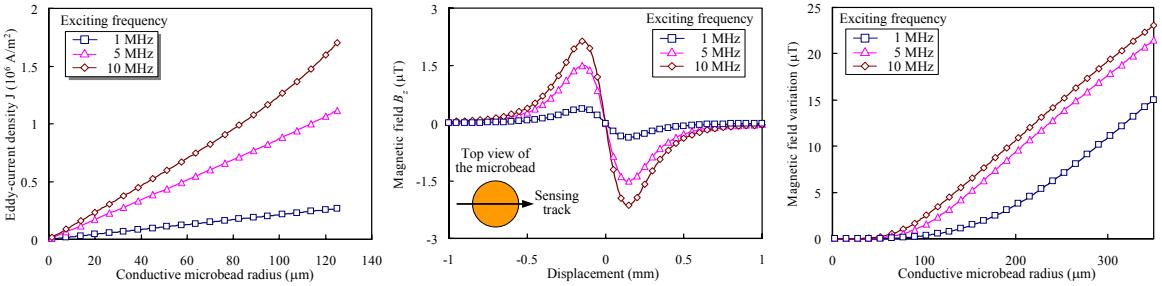

(a) Distribution of eddy-current density in microbead with 125 μm radius.

(b) Magnetic field B_z over sensing track on the microbead with 125 μm radius.

(c) Maximum magnetic field variation vs. microbead radius.

Figure 3: Analytical results of magnetic field occurred from eddy-current flowing in the microbead placed under uniform magnetic field B_0 = 100 μT and lift-off height of 162 μm.

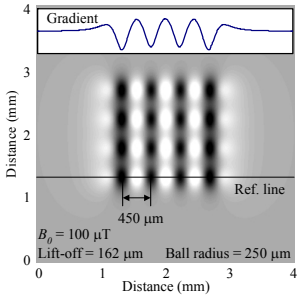

Figure 4: Simulation results of microbead array detection.

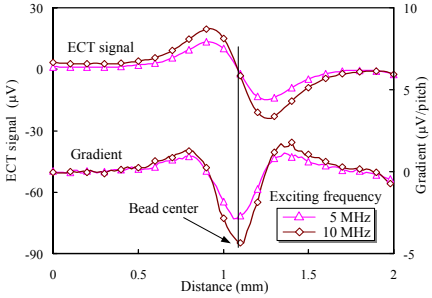

(a) ECT signal and its gradient.

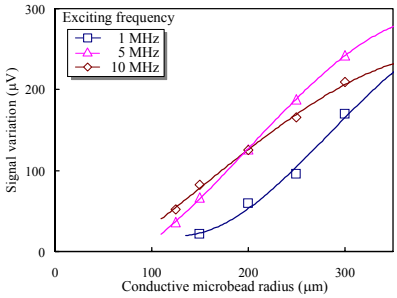

(b) Signal variation vs. microbead size.

Figure 5: Inspection signal obtained from SV-GMR sensor based on ECT technique

together by applying the Superposition theory as 2-D image shown in figure 4. The calculation results show the strong magnetic field distributions in z-direction produced from eddy currents flowing in microbead and verify the possibility of microbead array detection by ECT technique.

3.3 Recognition Results

The ECT probe scanned over the model with 20 μm scanning pitch and lock-in amplifier was used to measure the ECT signal obtained from SV-GMR sensor. The waveforms of ECT signal in figure 5(a) obtained from the detection of a microbead with 125 μm radius at the frequency of 5 and 10 MHz agree with the ECT signal waveforms obtained from analytical solution. Identifications of the microbead position are performed by considering the peak of ECT signal gradient. Figure 5(b) shows the maximum variation of the ECT signal versus the radius of the microbead ranged from 125 to 300 μm. The maximum signal variation at exciting frequency of 10 MHz decreases with the microbead radius and it is lower than the signal variation at exciting frequency of 5 MHz when the microbead radius is larger than 200 μm. This is because the planer meander coil can not generate the uniform magnetic field distribution. The experimental results also show that signal variations at the microbead depend on the frequency of the exciting magnetic fields and the microbead radius.

Numerical gradient technique applied to ECT signal enhances the signal at the microbead position to be easily recognized its position as shown in figure 6(a). In addition, the microbead pitches are also identified by considering the peak of the ECT signal gradient. The microbead array model with 125 μm radius and 410 to 460 μm microbeads pitches and its detection results are shown in figures 6(b) and 6(c) respectively. The microbeads are clearly recognized and the pitches of the microbead are also accurately specified with error less than 50 μm.

4 Ferromagnetic material detection

4.1 Experimental setup

As shown in figure 7(a), static magnetic fields around 100 mT were applied to ferromagnetic material to magnetize the ferromagnetic material. The SV-GMR sensor is also set the sensing axis to detect only the *z*-axis component of magnetic fields. Wheatstone bridge configuration as shown in figure 7(b) is used to eliminate the offset voltage. Distance between the SV-GMR sensor and ferromagnetic material is higher

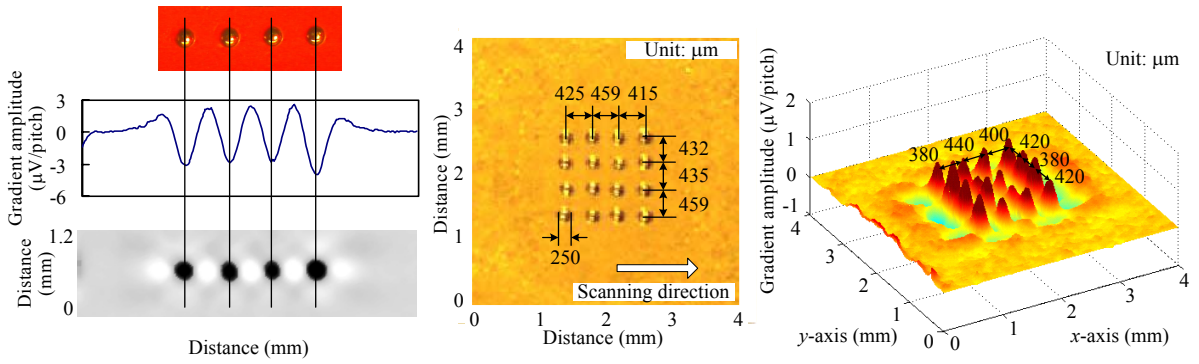

(a) Identification of microbead position (b) Ball grid array model (c) Detection results

Figure 6: Recognition of the microbead (PbSn) position, microbead (PbSn) array model and its detection results.

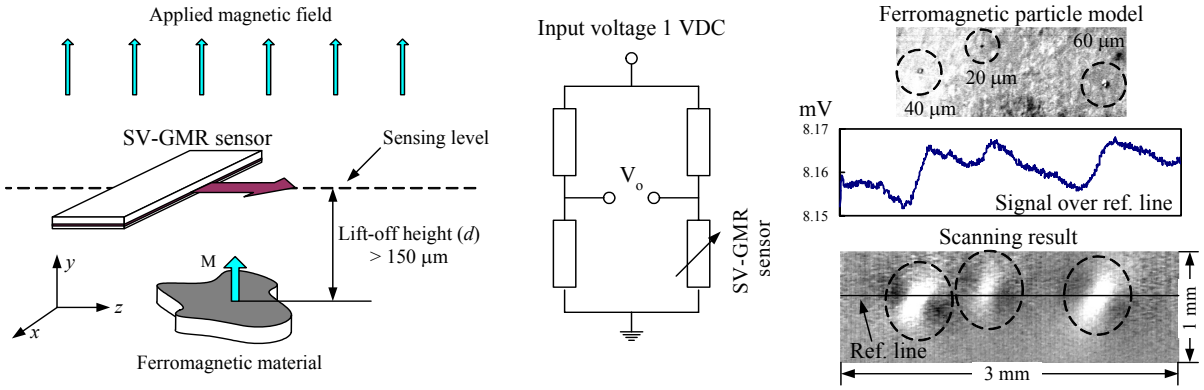

(a) Detection of ferromagnetic material (b) Electric circuit for ferro-magnetic material detection (c) Ferromagnetic material model and its recognition result

Figure 7: Simple model of ferromagnetic material (Fe) detection, Wheatstone bridge of SV-GMR sensor for ferromagnetic material detection, and example of ferromagnetic material recognition.

than 150 μm. The SV-GMR sensor is scanned over the ferromagnetic material with speed of 1 mm/min.

4.2 Recognition results

Figure 7(c) shows the ferromagnetic particle model and its recognition results. The ferromagnetic particle (Fe) with sizes between 20 to 60 μm was used as model. The signal over the ref. line shows the variation of signal wherever the ferromagnetic particle exists. The 2-D image obtained from scanning result is also shown that utilization of the SV-GMR sensor is able to detect the ferromagnetic particle clearly.

5 Conclusion

The analytical and experimental results showed that the SV-GMR can be applied to detect non-magnetic (conductive) material with size larger than 250 μm based on ECT technique. Moreover, the SV-GMR sensor can also be applied to detect ferromagnetic material with size larger than 20 μm. The results indicate that the SV-GMR is useful and possible to use in physical measurement and biosensor applications.

6 References

[1] Dogaru, T., Smith, S.T., "Giant magneto-resistance-based eddy-current sensor", *IEEE Trans. Maneticss.*, vol. 37, no. 5, pp 3831-3838, (2001).

[2] Wood, D.K., Ni, K.K., Schmidt, D.R., and Cleland, A.N., "Submicron giant magneto-resistive sensors for biological applications", *Elsevier sensors and actuators A*, vol. 120, issue 1, pp. 1-6 (2005).

[3] Anguelouch, A., Reich, D. H., Chien, C. L., and Tondra, M., "Detection of ferromagnetic nanowires using GMR sensoes", *IEEE Trans. Maneticss.*, vol. 40, no. 4, pp 2997-2999, (2004).

[4] Yamada, S., Chomsuwan, K., Fukuda, Y., Wakiwaka, H., and Shoji, S., "Eddy-current testing probe with spin-valve type GMR sensor for printed circuit board inspection", *IEEE Trans. Magnetics.*, vol. 40, no. 4, pp 2676-2678 (2004).

[5] Morisue, T., and Fukumi, M., "3-D eddy current calculation using magnetic vector potential", *IEEE Trans. Magnetics.,* vol. 24, pp. 106-109, (1988).